Investigating the Effect of Brake Parameters on Vehicle Dynamics for the Optimum Design

Morteza Mollajafari [1*], Javad Marzbanrad[2], Pooriya Sanaie[3]

[1] Assistant Professor, Vehicle Electrical and Electronic Research Lab, School of Automotive Engineering, Iran University of Science and Technology, Tehran, Iran

[2] Professor, Vehicle Dynamical Systems Research Laboratory, School of Automotive Engineering, Iran University of Science and Technology, Narmak, Tehran, Iran

[3] M.Sc. Student of Vehicle Electrical and Electronic Engineering, School of Automotive Engineering, Iran University of Science and Technology, Tehran, Iran

ARTICLE INFO	A B S T R A C T
	The braking system has always been considered one of the most significant vehicle subsystems since it plays a key role in safety issues. To design such a complex system, modeling can be a helpful tool for designers to save time and costs. In this paper, the hydraulic braking system of a B-Class vehicle was modeled by simulating the relationship between brake components such as pedals, boosters, main cylinders, and wheel cylinders, with the vehicle dynamics by using the existing models of the tire and their dynamic relationships. The performed modeling was compared with the results of a concerning vehicle's direct movement. The results of this comparison showed that our modeling is very close to the experimental data. The braking distance parameter was selected to examine the effects of each braking component on the vehicle dynamics. The results of investigating the effect of different parameters of the braking system on the dynamic behavior of the vehicle indicated that the main cylinder diameter, the diameter of the front and rear wheels' brake cylinders, the effective diameter of the front disk, and the diameter of the rear drum are the most effective design parameters in vehicle's braking system and optimal results are obtained by applying changes to these parameters.

1. Introduction

The braking system has always been considered one of the most important vehicle subsystems since it plays a key role in safety issues [1]. In recent years, there have been many improvements in the design of braking systems aimed at improving their performance and safety. Currently, designing braking systems for personal vehicles is among the most important needs of Iran, so localizing this knowledge is crucial to the achievement of this goal. The structure of velocity control tools found in automobiles was established decades ago and then summarized and described by Heisler [2]. Heisler showed that the hydraulic braking system is a compact method for transferring brake pedal force to any of the brakes on wheels by directing the fluid pressure from one position to another, converting the fluid pressure into useful work. in the wheels and finally reducing or stopping the wheels' rotation. Before recent advances in

Investigating the Effect of Brake Parameters on Vehicle Dynamics for the Optimum Design

electronics, modern vehicles used hydraulic fluid circuits to activate brakes. Similar to operating cables, mechanical brakes are interfaces mostly used for static applications such as hand brakes. The subsystem used for wheel brakes has been drum brake for many years. Drum brakes are made up of shoes and drums attached to the wheel. Disc brakes are the replacement for the drum brakes attached to the wheel and placed between the two pistons and the friction linings. Brake linings compress the disk surface. Since the introduction of this type of brakes, disc brakes are proven as suitable options for technology owners. They are used in almost all front axles of cars and heavy vehicles [3].Limpert has provided a complete and in-depth summary of the usual equations for designing and analyzing braking systems [4]. Equations that control variations in the thrust force of different tires during braking are of particular concern and important design methods are used to simulate the braking forces. Limpert defines the traction coefficient as the ratio of the braking force to the dynamic load of the axle. Choi et al (2008) [5] designed electrorheological (ER) controllable system for a pressure reducer valve and used it to control the distribution of braking forces in ABS braking systems. A cylindrical electrorheological valve was designed and its pressure controllability was verified experimentally. A hydraulic booster was also developed to reinforce the independent pressure drop due to the electrorheological valve and thus to obtain the governing equation on the rear wheel model. In this study, a sliding model controller was used to achieve the expected slide rate. Additionally, the animated results of the car's braking performance are shown unloaded mode. Hoi Peng et al (1996) [6], conducted research on optimizing the distribution of tire forces to maximize the acceleration / braking of the 4WDs while revolving. The purpose of this study was to investigate the expected improvement in the use of different steering and actuator mechanisms. Optimization is concerned with the simultaneous application of equal and unequal constraints using nonlinear programming methods. Hans Christoff et al. (1984) [7] studied the critical determinants for the addition of the optimal distribution of braking force in current and future scenarios. This research introduced an

ABS. A brief overview of the systems based on principles of adapted brake force distribution was presented in this paper. Discussions such as the control intervals of ABS dependent on the actual brake force distribution were discussed in this study. Bushman et al. (1992) [8] created electronic brake force distribution (EBD) as a subsystem of ABS to control the friction on the rear wheels. In this research, the pressure of the rear wheels was estimated with the ideal brake force distribution in partial braking operation. Common rear axle system and ABS components are presented in this paper. Yazdanpanah, R. and Mirsalim, M et al. (2014) reported the application of electromagnetic brakes as an acceleration-reducing piece in which friction brakes were less used and therefore never reached high temperatures [9]. The brake tubes had a long life and the potential risk of braking system failure could be eliminated. The new proposed mathematical model of electromagnetic brakes was shown to illustrate their static features (angular velocity vs. braking torque). The performance of the new mathematical model was better than other available models. The software program used to code the static and dynamic features of different brakes was written in MATLAB and their performance was evaluated on different roads [10].Kim et al (2007) [11] introduced the concept of vehicle stability control for a hybrid 4WD vehicle in which the regenerative energy of the rear brake and a hydroelectric brake was utilized. A genetic algorithm was used to achieve optimal brake torque distribution between regenerative brake and EHB torque. The genetic algorithm was used to calculate the optimal regenerative brake and EHB torques for given inputs, the desired yaw rate and the coefficient of friction. Based on the optimal distribution of the braking torque, the vehicle's stability control logic generates the optimum yaw torque to compensate for the lateral slide angle and yaw rate by the fuzzy control algorithm related to the steering angle and vehicle velocity [12]. Peter Franck et al (2000) [13] designed a control algorithm that calculated the 4WD braking forces to achieve an equal on two wheels. This slide control algorithm is applied in the small slide domain, where ABS is disabled. In the event of successful control, the wheels reach

3989   Automotive Science and Engineering (ASE)

the adhesion range at the same time that leads to ABS activation and the reduced high acceleration [14].Goodarzi et al. (2008) [15] investigated the optimization of ABS between the front and rear axles of trailers and improved the dynamic performance of these vehicles. The results of conducted studies in the field of modeling and simulation of the brake system indicate that it is crucial to identify important parameters. Therefore, the following sections attempt to investigate the effect of different parameters on braking dynamics by explaining the performance of braking components, while modeling and simulating them. Since determining the important parameters will play a significant role in optimizing the distribution of ideal forces, this article will address issue in detail.

2. The proposed method

The main components of the braking system are the pedal mechanism, the booster system, the main cylinder, the brake circuit and the wheels' cylinders. In this section, a brief description of the function and relationships between these components is provided.

2.1. Component of braking system

The first part addressed here is the brake pedal. In Fig. 1, the pedal, points of force application, the support and spring are shown.
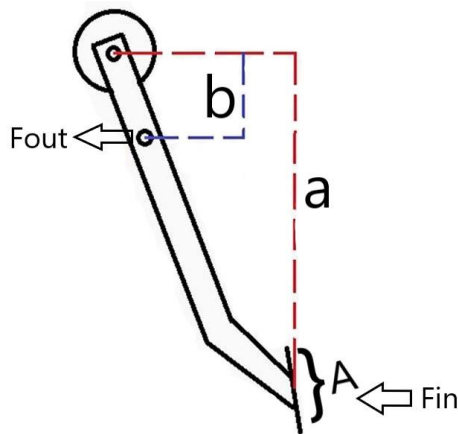

Figure 1: Braking pedal schematic

The shape, form, and movement of Figure 1 are determined. Among the forces and torques applied to the pedal, the forces applied to the pedal from the driver's foot and the force pushed by the pedal to the boosters are more important. The torque used to accelerate the angle of the pedal and overcome the restoring force is presented in the following relation:

$$F_{in} = \frac{aF_p - k_p\theta - I_p\ddot{\theta}}{b} \cong \frac{aF_p}{b} \quad (1)$$

2.1.1. Booster

The braking system booster uses engine power in various ways and increases braking power. Cars use the vacuum created by the engine's suction [16].

$$F_d' = \eta \times (A_d - A_{rod}) \times (P_{atm} - P_{manifold})(2)$$

$$F_d = F_d' - F_{sd} \quad (3)$$

In Eq.2, η is the booster efficiency (about 95%) and P_{atm} and $P_{manifold}$ are air and the engine inlet duct pressures respectively. F_{sd} The restoring force of spring is diaphragm and if the restoring force is deducted from F_d' force due to the pressure difference, the force reaching the booster output is obtained (Eq. 3). A_d and A_{rod} are the diaphragm and rod areas of load application. As no force is applied to the rod surface because of the air pressure, this area is deducted from the diaphragm area. The force spent to overcome the spring is reduced. The remainder of the force acting on the reaction disc acts as a fluid under pressure and its pressure is determined by relation (4). In this case, this pressure is provided by the force applied to the booster. This force is summed up with the force that is used to retract the valve springs.

$$P_{disc} = \frac{F_d}{\frac{\pi(D_o^2 - D_i^2)}{4}} \quad (4)$$

$$F_{in}' = \frac{\pi D_i^2}{4} \times P_{disc} \quad (5)$$

$$F_{in} = F_{in}' + F_{s1} + F_{s2} \quad (6)$$

D_o is outer radius and D_i inner radius, F_{s1} and F_{s2} are the restoring forces of two booster valves. The total force is obtained by summing the restoring forces and the force applied to the piece. The booster coefficient is obtained from the following equation.

Investigating the Effect of Brake Parameters on Vehicle Dynamics for the Optimum Design

$$B = \frac{F_{out}}{F_{in}} \cong \frac{F_d + F_{in}}{F_{in}} = \frac{F_d + A_i \times \frac{F_d}{A_o - A_i}}{A_i \times \frac{F_d}{A_o - A_i}}$$
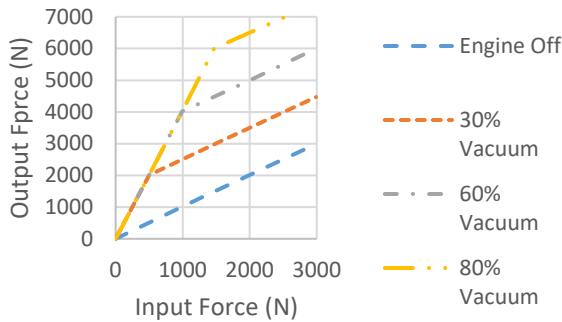
$$= \frac{A_o}{A_i} \quad (7)$$

Figure 2: Booster parameters effect on output force

2.1.2. Main Cylinder

In the main cylinder, the fluid pressure in the chamber is obtained with the force behind the piston and the cross-section of the cylinder.

$$P = \frac{F_{mp}}{A_{mc}} \quad (8)$$

A_{mc} is area of main cylinder and F_{mp} is force that applied to the main piston. However, Force and pressure, however, can change depending on certain factors. The force entering the booster is subject to some drops after being boosted. Some of these drops are associated with the forces spent on retracting the booster springs as well as the ones created by friction. When the boost output force is introduced into the first piston and the friction is overcome, the piston accelerator force and its restoring force increase the pressure in first path. The same situation is true for the second path. A series of drops such as friction inside the tubes will reduce pressure on the second path as well.

2.1.3. Disk brake

Brake relations in wheels can be examined from two perspectives, one is the braking torque in terms of the inlet pressure and the other one is the effect of the brake pressure on the brake components. In the cylinder of wheels, the force behind the lining F_a is equal to:

$$F_a = A_{wc} \times P \quad (9)$$

r_{eff} is the effective radius of the disk and μ is the coefficient of friction between the lining and disk. The brake factor is the ratio of tensile force on the engine to the vertical force of the lining. In disc brakes [17]:

$$B.F. = 2\mu \quad (10)$$

In studies and experiments, it has been demonstrated that the main change due to applying disc brake pressure is due to the compression of the brake linings, which are softer than the disk or caliper. The brake caliper is also deformed due to the applied force and braking pressure.

2.1.4. Drum brakes

In drum brakes, there are a variety of modes depending on the position of the shoe and location of the force applied to the shoe [18].

$$\boldsymbol{T_b = F_a \times B.F. \times r_{drum}} \quad \textbf{(11)}$$

Other necessary relationships in a shoe brake are the effects of brake pressure on different components, which are obtained by experiments and experience similar to disc brakes. Major changes in brake fluid volume are due to filling of the gap between the lining and drum. This is due to shoe and lining deformation and volume change Other necessary relationships in a shoe brake are the effects of brake pressure on different components, which are obtained by experiments and experience similar to disc brakes. Major changes in brake fluid volume are due to filling of the gap between the lining and drum. This is due to shoe and lining deformation and volume change the heating of the drum [19].

$$\Delta V_{clearance} = 0.14 \times A_{wc} \quad (12)$$

$$\Delta V_{drum} = k_d A_{wc}^{\;2} p_L \quad (13)$$

$$\Delta V_{shoe} = \frac{k_s A_{wc}^2 p_L}{dw} \quad (14)$$

$$\Delta V_{thermal} = 3.14 \alpha_t dT_d A_{wc} \quad (15)$$

The above-mentioned factors are presented on the left side of the above relations and the rest of quantities include A_{wc} (wheel cross-sectional area), p_L (brake fluid pressure), d (drum diameter), w (lining width), T_d (drum temperature), and α_t (expansion coefficient). The coefficients k_s varies in the ranges of 100×10^{-6}- 150×10^{-6} in cm^3/N and 20×10^{-4} - 30×10^{-4} in cm/N.

2.2. Braking System Modeling

In modeling and optimization, the important point is the relationship between various variables affecting the tire. Different models are presented for tire through conducting experiments and empirical and theoretical methods. Some of the more famous ones include Fiala [20], Pacejka [21], Dugoff [22] and other models. Given the accuracy and efficiency of each of the mentioned models, the Pacejka tire model was selected as the model for simulating the dynamic behavior of the braking system.

2.2.1. Pacejka tire model

This model is the most comprehensive tire model introduced in 1989 and its new versions include Pacejka89, Pacejka94, Pacejka96 and etc. In this method, there are coefficients b_0 to b_{10} to calculate the longitudinal force, a_0 to a_{13} to calculate the transverse forces and other coefficients for characteristics such as the restoring torque for each tire. These coefficients are different for each tire.[23]

$$C = b_0 \quad (16)$$

$$D = (b_1 \times F_z^2 + b_2 \times F_z) \quad (17)$$

$$BCD = (b_3 \times F_z^2 + b_4 \times F) \times e^{(-b_5 \times F_z)} \quad (18)$$

$$B = BCD/(C \times D) \quad (19)$$

$$S_h = b_9 \times F_z + b_{10} \quad (20)$$

$$S_v = 0 \quad (21)$$

$$X_1 = \kappa + S_h \quad (22)$$

$$E = (b_6 \times F_z^2 + b_7 \times F_z + b_8) \quad (23)$$

$$F_x = (D \times sin(C \times Arc\,tan(B \times X_1 - E \times (B \times X_1 - Arc\,tan(B \times X))))) + S_v \quad (24)$$

In the above relations, F_x, F_z and F_y are the longitudinal, vertical and transverse forces in KN. K is the longitudinal slide coefficient where S_h and S_v are vertical and horizontal distances of force points from the center of the contact area. With the above information, Fig 3. below shows its longitudinal force in terms of different vertical loads and slip ratio.
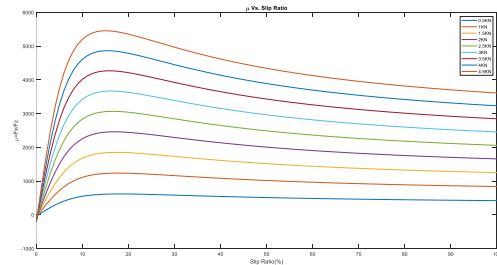

Figure 3: longitudinal force in terms of different vertical loads and slip ratio

Although Pacejka is a precise model, it has problems, one of which is the multiplicity of coefficients that make achieving them through experimental means time-consuming and expensive. In this paper, the Pacejka model has been used with data obtained for a sample car.

2.2.2. Modeling pedal input

Investigating the Effect of Brake Parameters on Vehicle Dynamics for the Optimum Design

It is better to have the pedal input, the force applied to pedal and its function relative to time similar to what happens in the test curve. Such a function grows exponentially and then reaches a constant value i.e. the loss of forces at the end of the braking action caused by the driver's sense is ignored. In this modeling, f_{max} as the final force and τ as time constant, which depends on the driver's braking, are required as the basic information.

$$f = f\left(\frac{1}{1 + 100e^{-t/\tau}} - \frac{1}{101}\right)_{max} \quad (25)$$

During braking, in addition to boosting pedal force and using energy to move other braking components, the energy of the driver's foot will be spent on two other tasks i.e. overcoming the inertia of the pedal and force or the torque of the spring bringing the pedal back $K_p\theta$. The MATLAB model of the pedal has been shown in figure 4.
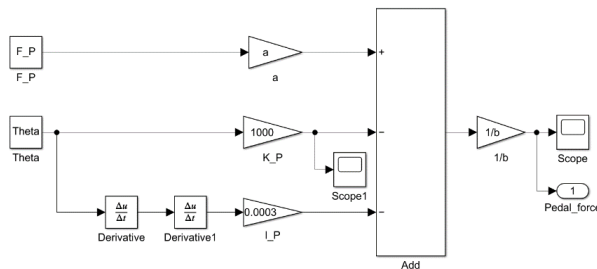

Figure 4: Pedal Model in Braking System

The input force is applied to the pedal model. This force is multiplied by the arm a and turned into the applied torque. The spring torque (i.e. the change in angle of the pedal in the torsional stiffness of pedal spring) is deducted from this quantity and then the torque required to overcome the inertia obtained by multiplying the angular acceleration of the pedal with rotational inertia is deducted as well. The remaining torque is converted to force by converting the pedal arm (multiplied by 1 / b) and then applied to the next part. The below formula is showing the pedal

force and input force relationship for the next part.

$$F_{in} = \frac{aF_p - K_p\theta - I_p\ddot{\theta}}{b} \cong \frac{aF_p}{b} \quad (26)$$

In the brake dynamical system, the brake components act as a capacity element (spring) and with force and pressure in hand, the displacement can be achieved finally. Therefore, derivation is used to obtain acceleration, which is not desirable due to potential instability; however, this procedure is taken and no problem arises. The acceleration coefficient of the pedal in the mode shown is almost a/b, because the restoring and inertia forces are small relative to the pedal output force. In addition, dry friction torque in the pedal hinge is so low that it is neglected in modeling.

2.2.3. Modeling the vacuum booster

The component after pedal in the braking system is the driver's feet power boost, which uses engine energy for this purpose. In the model, a vacuum booster, the software model of which is presented in Figure 5, is made using booster characteristics.
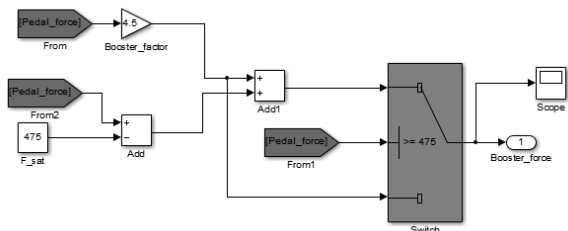

Figure 5: Vacuum booster model

The conventional booster is modeled on most cars that are located next to the pedal and along the push rod. In this model, a Master Vacuum booster is used. In above figure, it can be seen that the booster has its own boost before it is saturated, and after saturation, the boost factor will be one. The booster input force is a factor of pedal force (pedal ratio), and the brake circuit

3993   Automotive Science and Engineering (ASE)

pressure is the coefficient of output force (the main cylinder cross-section). Therefore, in the booster model, depending on the shape of the output curve in relation to the input, the output booster force is determined. The value spent on the acceleration of the objects inside the booster and the retraction of the spring is deducted from this force (booster springs are located after the booster plate).
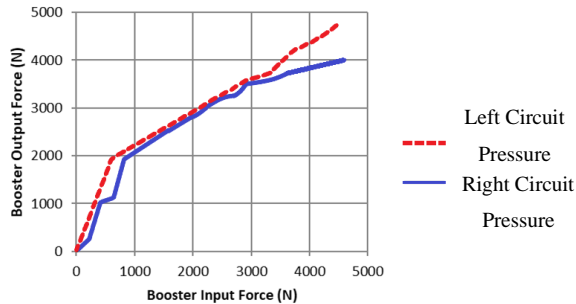

Figure 6

2.2.4. Modeling the main cylinder

The main cylinder is located after the booster and the booster output force is applied to it. In the braking model, the Tandem Master Cylinder is modeled. In both chambers, the force used to accelerate the first piston and the force required to retract the first spring are subtracted from the force applied to the first piston, and the output of this part is a force that applied pressure to the first chamber. Similarly, to the first set of forces, by deducting the forces as in the previous set of forces, the force of the second chamber and pressure of the second path are calculated. In Figure 7, the master cylinder model is shown in terms of its specific parameters.
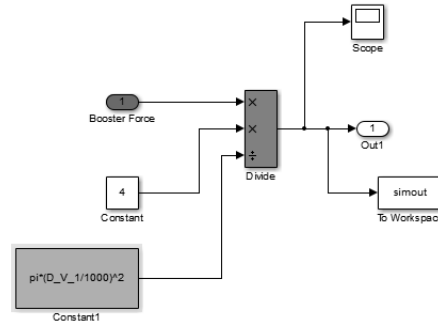

Figure 7: Main Cylinder Model

2.2.5. Modeling the wheel brakes

Disc brakes and the elements that consume a bulk of brake fluid when applying pressure are discussed in this section. Major changes occur in volume in the hose, tube, deformation in the caliper and compression of the lining. To find the stiffness coefficient of these springs (the ratio of pressure to volume change), the relations presented in the previous sections are used.

$$v_i = \sum p_i k_i \quad (27)$$

The pressure p_1 in addition to changing the volume in the components is multiplied by the cross-section of the cylinder and the force applied to the linings. After multiplying this force with the brake factor and effective radius of the disc, the torque applied from the braking system to the rotating parts with the wheel are obtained. However, this torque is a function of the angular torque of the wheel, the velocity of the vehicle and the longitudinal forces applied on the wheel. In other words, the coefficient of friction between the lining and the disc in the wheel rest mode varies between the zero and its maximum value at the threshold of movement. Hence, in the case of specified angular acceleration, such as in the case of zero angular acceleration in the resting mode, longitudinal forces determine the applicable braking torque and there will be no braking torque in the absence of longitudinal force; however, there is a pressure behind the brake pistons. In the model, given that the

Automotive Science and Engineering (ASE)   3994

experiments are carried out in a smooth field the longitudinal forces are only equal to the product of the vertical force in the coefficient of friction, and there is no other longitudinal force such as the force due to the gradient of the ground. The torque resulting from this longitudinal force $R_w F_x$ and the torque from the braking system T_b determine the wheel angular acceleration.

$$T_b - R_w F_x = I\alpha \quad (28)$$

Where, I is the rotational inertia of the wheel and its attachments and α is the declining angular acceleration. The amount of braking torque and angular acceleration are considered positive.

$$T_b = P_i \times A_{wc} \times B.F. \times r_{eff} \quad (29)$$

The angle and displacement of the pedal and booster are obtained by change in the size of the brake components.

$$pedal\_travel = \frac{\sum v_i}{A_{mc}} \times \frac{a}{b} \quad (30)$$

The output of each brake component is the brake torque and the volume of brake fluid used in that wheel. This is obtained by total consumed volumes and volume of displacement of the brake fluid. The displacements of the cylinder and booster components as well as the displacement of the pedal angle are obtained by dividing this volume by the main cylinder area.

2.2.6. Modeling the dynamics of the vehicle

In this section, using the longitudinal force and torque, the angular acceleration of the wheels is obtained. Based on the initial value of the velocity, the angular acceleration of the wheels is obtained. Then, with the help of two angular velocities of both wheels and velocity of the vehicle, the longitudinal slide is calculated separately for each wheel [24].

$$slip = \frac{v - r\omega}{v} \quad (31)$$

v is the velocity of the vehicle is in meters per second, r is the effective radius of the wheel in meters and ω is the angular velocity in radians per second. After obtaining the coefficient of friction (from the slide curves), using the vertical force of each wheel, the longitudinal force of each wheel is obtained, which causes braking and deceleration, or stopping the vehicle. These forces result in the acceleration of the car during braking. That is, the algebraic sum of the longitudinal forces is calculated, which results in the vehicle's longitudinal acceleration (newton's law).

$$a = \frac{\sum F_x}{m} \quad (32)$$

After integrating this acceleration and given the initial velocity applied to the system, the velocity of the vehicle is obtained as a function of time.

$$v(t) = \int_0^t a(t)\,dt \quad (33)$$

Reintegration of velocity results in the traversed distance since the moment of braking.

$$d(t) = \int_0^t v(t)\,dt \ , \ \ d(0) = 0 \quad (34)$$

3. Analysis and interpretation of results

In this section, the results of simulation and modeling in the previous sections will be presented and discussed. A model that represents the braking system of a sample vehicle whose information is given in table 1, is tested and the results related to the implementation and automotive dynamic system is achieved.

No.	Parameter	symbol	value	unit
1	Mass	m	850	Kg
2	Pedal Maximum Force	$fmax$	500	N
3	Friction Coefficient	μ	0.41	-
4	Vehicle length	l	2355	mm

5	Vehicle width	t	1400	mm
6	Gravity center height from Ground	h	546	mm
7	Front axle distance to gravity center	lf	873	mm
8	Vehicle rotational inertia	I	1000	Kg.m²
9	Pedal length	a	311	mm
10	Pedal length	b	73.8	mm
11	Front wheel rotational inertia	If	0.6	Kg.m²
12	Rear wheel rotational inertia	Ir	0.4	Kg.m²
13	Wheel radius	rw	262	mm
14	Master cylinder diameter	Dmc	19.05	mm
15	Front Brake Cylinder diameter	$Dwcf$	48.1	mm
16	Front Brake Disc diameter	Df	180	mm
17	Rear Brake Drum diameter	Dr	170	mm
18	Rear Brake Cylinder diameter	$Dwcr$	15.78	mm
19	Booster Factor	BF	4.5	-

Table 1: sample vehicle whose information

3.1. Model validation

Using the experimental results of Levin [25] on the sample vehicle, the details of which can be found in the previous section, will make the model reliable and allow it to be used instead of actual testing or optimization. Information and assumptions related to experiment are as follows:

I.   A sample vehicle with front and rear disc brakes is tested.

II. In all cases, braking is done after clutching.

III. The experiment on the dynamometer in which the tangential force component of the wheel can be measured in different pedal forces

To compare the experimental results and the results of road tests, the initial velocity is taken as 60km/h and the pedal force is 300N.
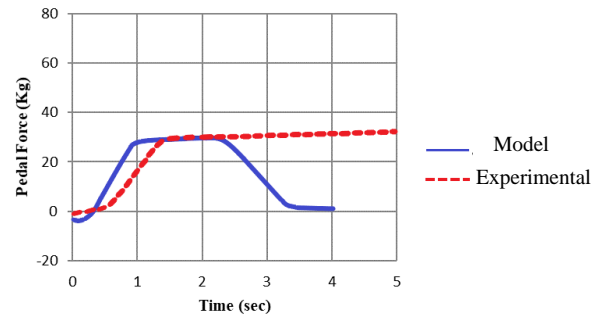

Figure 8

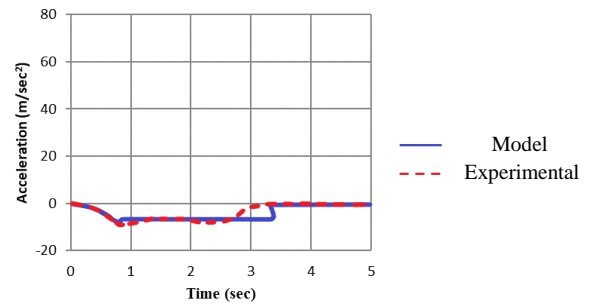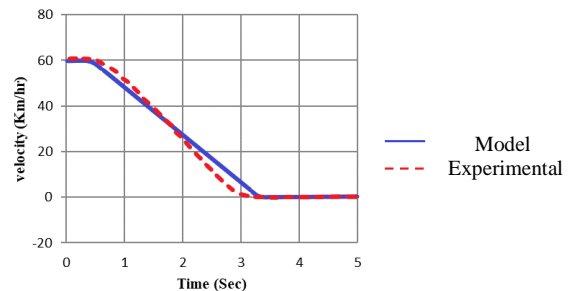In Fig. 8 pedal force is shown in experimental and modeled.

Figure 9

Figure 10

Investigating the Effect of Brake Parameters on Vehicle Dynamics for the Optimum Design
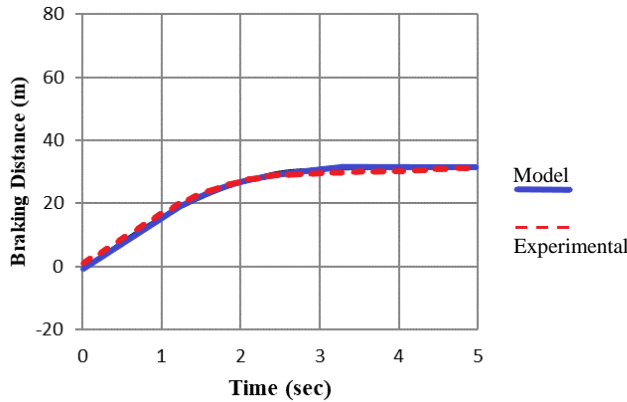

Figure 11

According to the above diagrams, the results of the modeling are consistent with those obtained in the experiments. Consequently, the results of this modeling can be used to evaluate the dynamic behavior of the braking system in a B-Class vehicle.

3.2. Effect of braking system parameters

Pedal input is the first and most important parameter determining the brake behavior. Driver can apply any input to the pedal depending on the ability he has and this feature is independent from the brake components. This feature mostly depends on the driver. Below is a braking simulation with different pedal inputs for a sample car. Other factors are constant in two modes: velocity in both modes is 35 km/h.
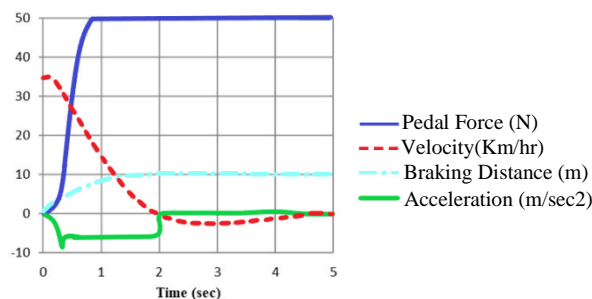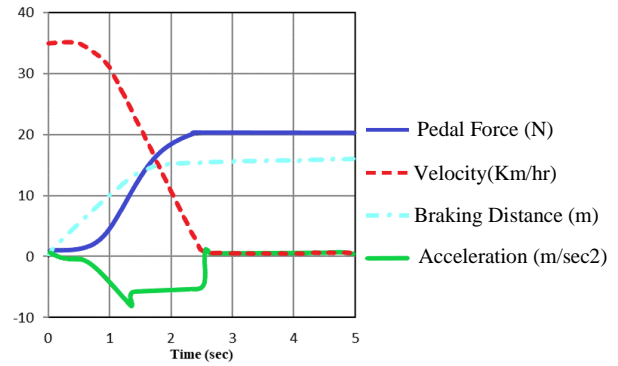

Figure 12

Figure 13

As a result, if the car brakes slowly, it will stop after 2.5 seconds, while if it breaks severely, it will stop after 1.8 seconds. An important member that plays a decisive role in the design of the braking system is the booster. The software model with a booster has a boost factor of 4.5 and the saturated force of 450 N is implemented. With the same features, the model has been implemented in the off-mode of the engine and in the absence of booster. The results are shown in Figure 14 Figure 15.
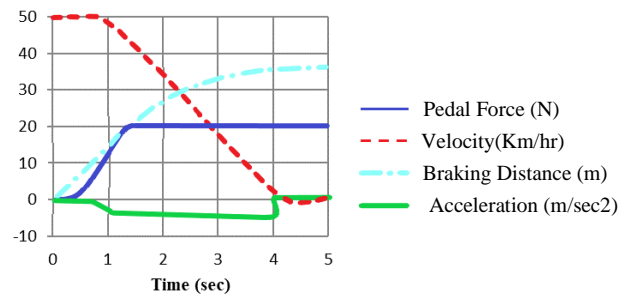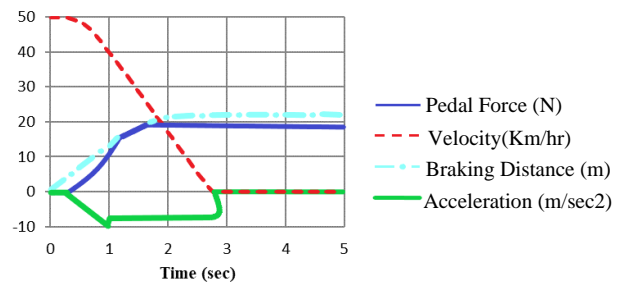

Figure 14

Figure 15

3997   Automotive Science and Engineering (ASE)

By changing the features of the braking system, a number of quantities related to the behavior of the car during braking change. Brake acceleration, wheel angular acceleration, wheel slide coefficient and brake line indicate brake status.

The brake distance has been chosen among the important quantities in the braking test. In the simulation of braking, the distance that the vehicle travels from the moment of braking until it stops, is achieved by double integrating the acceleration of the vehicle with respect to the initial velocity and other conditions. This quantity resembles the system performance. Firstly, the changes in this quantity are very mild compared to time. This is because they do not suffer from the variations and instability of quantities such as vehicle acceleration or the angular acceleration of the wheels. This advantage is due to the integrators' features in mechanical, electrical or software systems. On the other hand, this quantity, as specified in the brake standards, [3] provides a good understanding of the braking state to the designer or braking optimizer. According to the discussed issues, the parameters' effects are now examined. The quantity that can be changed easily and linearly is the main brake cylinder. The diameter of the cylinder and the main piston determines the amount of pressure on brake fluid by the applied force .As the cylinder diameter increases, the brake pressure is reduced and the braking force is lowered. Figure 17 shows the variations in the length of the brake line relative to the variations in the main cylinder diameter with multiple inputs for the sample vehicle.
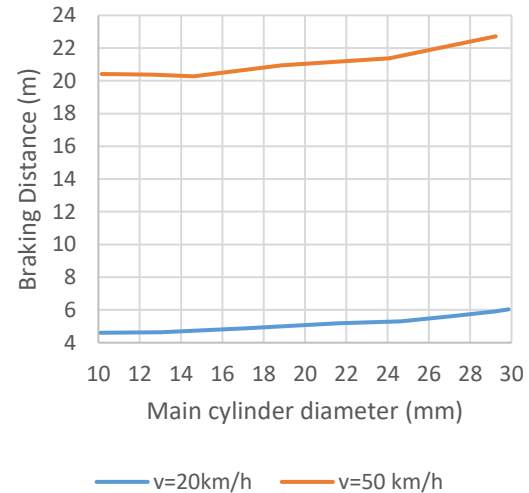

Figure 16: Brake distance in different cylinder diameters at two different velocities

In above figure, it is observed that with increasing cylinder diameter, the length of the brake line increases. The cylinder diameter of the sample vehicle is 19.05 mm. The simulation data in Figure 15 shows that the required length of the brake line is satisfied with the applied diameter. The next important component that is selected from the front brake features. After converting the force into pressure, the factor determining the amount of force applied to the linings is the cross-sectional diameter of the wheel cylinder. In Figure 17, the change in brake distance is plotted vs. the change in the diameter of the front-wheel brake cylinder of the sample vehicle.

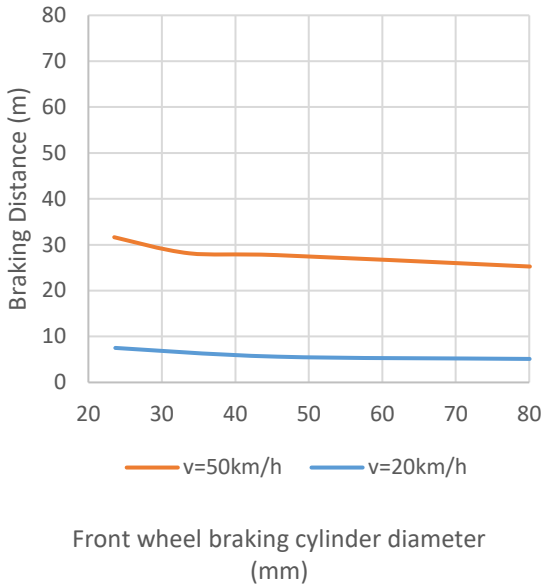# Investigating the Effect of Brake Parameters on Vehicle Dynamics for the Optimum Design

Figure 17

The diameter of the front disk is also involved in the length of brake line and these changes are presented in Figure18.
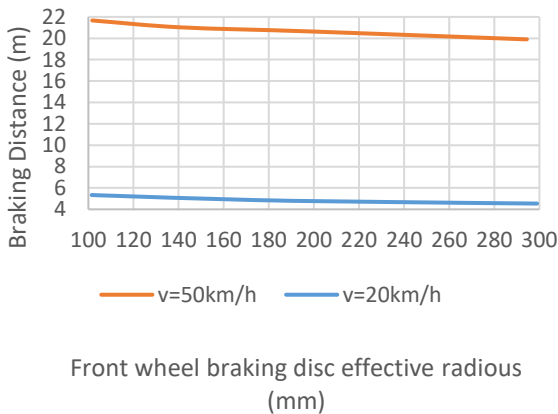

Figure 18

Based on the rear brake, the effect of changes in two features on the braking behavior (length of the brake line) has been investigated. There are two dimensions to pay attention to: the diameter of the rear-axle brake cylinder and the wheel drum diameter. In Figure 19 and Figure 20, the effect of changes in these two parameters has been investigated.
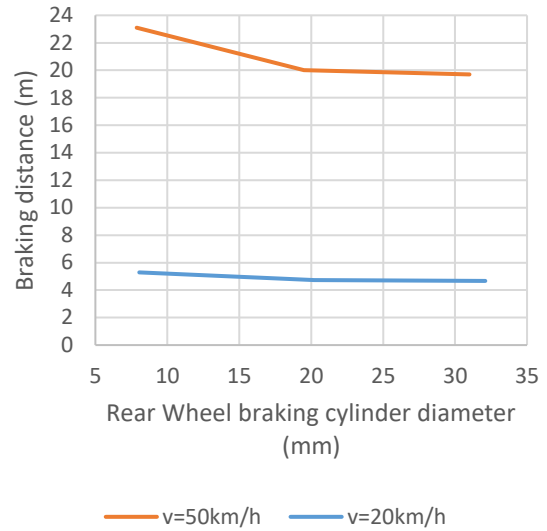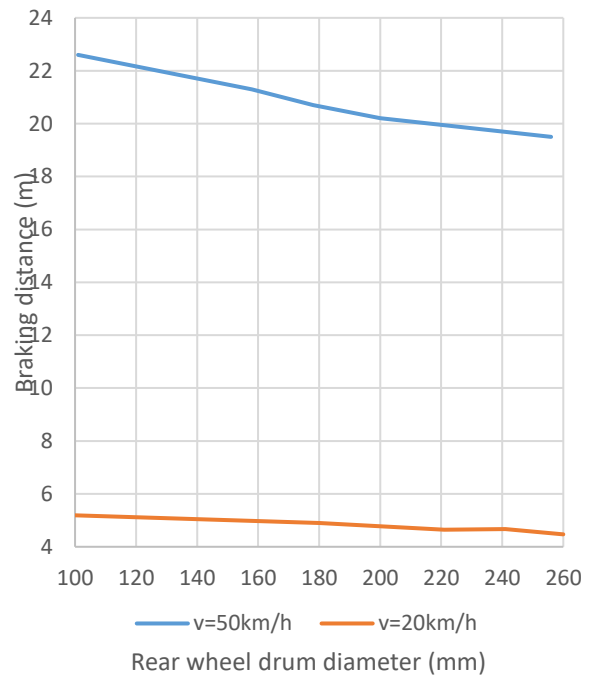

Figure 19

Figure 20

To use the charts of Fig. 18-22, each of the features is the amount used in the vehicle. The front axle brake cylinder diameter is 48.1 mm. Given that the force applied to the disk is proportional to the cylinder area and its second power diameter, it is observed that the length of the brake line decreases with increasing the

3999   Automotive Science and Engineering (ASE)

cylinder diameter parabolically. As the power and weight transfer of the front axle are higher than the rear axle, the wheels of this axle will be locked up later. This is because the cylinder area will be followed by increasing braking power and reducing the length of the brake line. As increasing the cylinder's diameter causes the wheels to lock on the rear axle, the diagram shows that this occurs at diameters more than 20 mm in the rear cylinder. However other than increasing braking power and lowering the braking distance, there are other constraints in the design. For example, due to the increase in cylinder diameter, the pedal movement also increases because when the pedal moves, the brake fluid moves in the larger cylinder (Fig. 22).
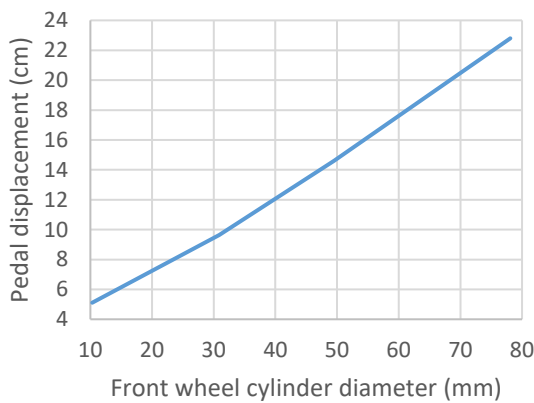

Figure 21

Now, based on the cylinder diameter of the sample car in Figs. 19 and 23, it is concluded that the applied diameter is appropriate. Figure 19 also shows that braking power increases with disk diameter. The brake torque has a direct relation to the effective radius of the disc. For this reason, disc diameter changes affect the length of the brake line almost linearly. On the other hand, increasing the outer diameter of the disk has other limitations. The blank space of the ring is where the disk is placed. In the sample car, the inner diameter of the ring is 278 mm. The diameter of 219 mm and the effective diameter of 180 mm are satisfactory as shown in figure 20. The same

limitation exists in the case of the rear axle. Due to the outer diameter of the drum, the applied size meets the brake line requirements. In line with the front wheel's cylinder diameter, the rear wheel's cylinder diameter has a great influence on the wheel's brake torque, however due to the low vertical force on the rear axle during braking, with increasing cylinder diameter and enhancing braking torque, the rear wheel becomes locked and not only braking force does not increase but actually decreases. Figure 21 shows that in the diameters more than 20 mm for the rear wheel cylinder, the brake line is almost constant. In this section, the effect of changing another parameter is also examined. The coefficient of friction between the linings and the risk or rear wheel drum depends on their material. Discs and drums are often steel. This coefficient changes due to changes in temperature and atmospheric conditions and wearing.
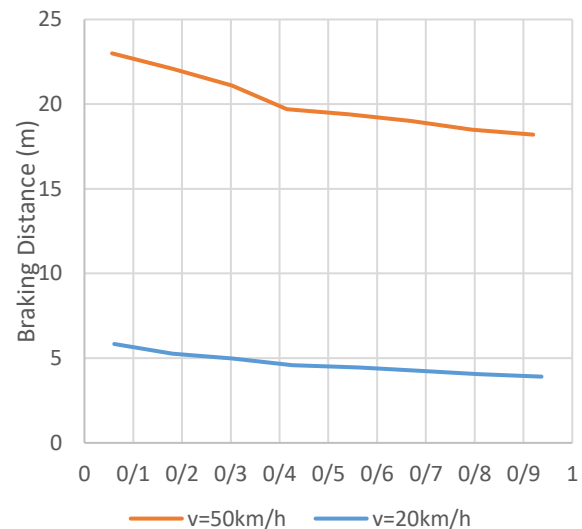

Figure 22: Friction coefficient between braking pads and disc or drum

Although the above diagrams are based on the results of the software model, they resemble the car's behavior based on reality. The above graphs (the coefficient of friction is 0.41) also show that the car brake is not heated in the normal state. In this situation, experiments show that the length of

Automotive Science and Engineering (ASE)   4000

the brake line is 15.30 at 40 km/h and 30.6 at 60 km/h.

4. Conclusions

Braking system modeling can be a helpful for designers to save time and costs. The hydraulic braking system of a B-Class vehicle was modeled by simulating the relationship between brake components such as pedals, boosters, main cylinder and wheel cylinders, vehicle dynamics and using existing models for tire and dynamic relationships. The performed modeling was compared with the results of an experiment on direct vehicle movement. The results of this comparison showed that the modeling was very close to the experimental data. The brake distance parameter was selected to examine the effects of each braking system on the vehicle dynamics. The results of investigating the effect of different parameters of the braking system on the dynamic behavior of the vehicle indicated that the main cylinder diameter, the diameter of the front and rear wheels' brake cylinders, the effective diameter of the front disk and the diameter of the rear drum are the most important design parameters in vehicle's braking system and optimal results are obtained by applying changes to these parameters.

4. References

[1] Vaa, T., Penttinen, M., & Spyropoulou, I. (2007). Intelligent transport systems and effects on road traffic accidents: state of the art. IET Intelligent Transport Systems, 1(2), 81-88.

[2] Heisler, H. (2002). Advanced vehicle technology. Elsevier.

[3] García-León, R.A. and Flórez-Solano, E., 2017. Dynamic analysis of three autoventilated disc brakes. Ingenieria e investigacion, 37(3), pp.102-114.

[4] Limpert, R. (2011). Brake design and safety. SAE international

[5] Choi, H.S., Lee, W.J., Park, M.N. and Kim, E.T., 2008. Design Of Adaptive Sliding Mode Control For Aircraft Anti-braking System. In Proceedings of the IEEK Conference (pp. 1083-1084). The Institute of Electronics and Information Engineers.

[6] Peng, H. and Hu, J.S., 1996. Traction/braking force distribution for optimal longitudinal motion during curve following. Vehicle System Dynamics, 26(4), pp.301-320.

[7] Becker, W., Janssen, R., Mueller-Hellmann, A., & Skudelny, H. C. (1984). Analysis of Power Converters for AC-Fed Traction Drives and Microcomputer-Aided On-Line Optimization of Their Line Response. IEEE Transactions on Industry Applications, (3), 605-614.

[8] Buschmann, G., Ebner, H., and Kuhn, W., "Electronic Brake Force Distribution Control - A Sophisticated Addition to ABS," SAE Technical Paper 920646, 1992, https://doi.org/10.4271/920646.

[9] Yazdanpanah, R. and Mirsalim, M., 2014. Hybrid electromagnetic brakes: design and performance evaluation. IEEE Transactions on Energy Conversion, 30(1), pp.60-69.

[10] Tyan, F., Hong, Y.F., Tu, S.H. and Jeng, W.S., 2009. Generation of random road profiles. Journal of Advanced Engineering, 4(2), pp.1373-1378

[11] Kim D-H, Kim J-M, Hwang S-H, Kim H-S. Optimal brake torque distribution for a four-wheeldrive hybrid electric vehicle stability enhancement. Proceedings of the Institution of Mechanical Engineers, Part D: Journal of Automobile Engineering. 2007;221(11):1357-1366. doi:10.1243/09544070JAUTO352

[12] Kim, D. H., Kim, J. M., Hwang, S. H., & Kim, H. S. (2007). Optimal brake torque distribution for a four-wheeldrive hybrid electric

vehicle stability enhancement. Proceedings of the Institution of Mechanical Engineers, Part D: Journal of Automobile Engineering, 221(11), 1357-1366.

[13] Mollajafari, M. and Shojaeefard, M.H., 2021. TC3PoP: a time-cost compromised workflow scheduling heuristic customized for cloud environments. Cluster Computing, 24(3), pp.2639-2656.

[14] Shahhoseini, H.S., Saleh Kandzi, E. and Mollajafari, M., 2014. Nonflat surface level pyramid: a high connectivity multidimensional interconnection network. The Journal of Supercomputing, 67, pp.31-46

[15] Avesta Goodarzi, Mohammad Behmadi & Ebrahim Esmailzadeh (2008) An optimised braking force distribution strategy for articulated vehicles, Vehicle System Dynamics, 46:sup1, 849-856, DOI: 10.1080/00423110802037107

[16] Day, A.J. and Bryant, D., 2022. Braking of road vehicles. Butterworth-Heinemann.

[17] Mollajafari, M. and Shahhoseini, H.S., 2011. A repair-less genetic algorithm for scheduling tasks onto dynamically reconfigurable hardware. International Review on Computers and Software, 6(2), pp.206-212.

[18] Stone, R. and Ball, J.K., 2004. Automotive engineering fundamentals. SAE International.

[19] Halderman, J.D. and Mitchell, C.D., 2004. Automotive brake systems. Pearson/Prentice Hall.

[20] Jiang, Y., Wu, P., Zeng, J., Wu, X., Zhang, Y., Yang, Z., ... & Dai, X. (2021). Researches on the resonance of a new type of suspended monorail vehicle-bridge coupling system based on modal analysis and rigid-flexible coupling dynamics. Vehicle System Dynamics, 59(1), 135-154.

[21] Pacejka, H. (2005). Tire and vehicle dynamics. Elsevier.

[22] Ding, N. and Taheri, S., 2010. A modified Dugoff tire model for combined-slip forces. Tire Science and Technology, 38(3), pp.228-244.

[23] Guiggiani, M., 2014. The science of vehicle dynamics. Pisa, Italy: Springer Netherlands, 15.

[24] Gillespie, T. ed., 2021. Fundamentals of vehicle dynamics. SAE international

[25] Mohtavipour, S.M., Mollajafari, M. and Naseri, A., 2020. A novel packet exchanging strategy for preventing HoL-blocking in fat-trees. Cluster Computing, 23, pp.461-482.